



Ruthenium hydroxide supported on activated alumina for catalytic permanganate oxidation of aniline

Jing Zhang^{a,*}, Ruijia Zhang^a, Ying Gao^{a,b}, Ying Zhang^c

^aKey Laboratory of Integrated Regulation and Resource Development on Shallow Lakes, Ministry of Education, College of Environment, Hohai University, Nanjing 210098, China, Tel. +86 15050556980; email: zhang_jing@hhu.edu.cn (J. Zhang), Tel. +86 15295526603; email: ruijia233@163.com (R. Zhang), Tel. +86 18936038266; email: seesmile@163.com (Y. Gao)

^bCollege of Mechanical and Electronic Engineering, Hohai University, Changzhou 213022, China

^cCSCEC AECOM Consultants Co. Ltd, Beijing 100044, China, Tel. +86 13811459248; email: zlk_yxc@163.com

Received 28 December 2014; Accepted 14 August 2015

ABSTRACT

Ruthenium loaded on CeO₂ or TiO₂ has been proved to be effective catalysts in permanganate oxidation, but the small size of supports led to a difficult separation of catalysts from the aqueous solution. Therefore, ruthenium hydroxide supported on activated alumina (diameter 3–4 mm), i.e. Ru-AA, was synthesized and employed as catalyst in permanganate oxidation of aniline at circumneutral pH for the first time. The characterization for Ru-AA by SEM-EDAX proved the existence of Ru on the surface of AA, but XRD patterns for AA were not affected by the impregnation of ruthenium hydroxide, due to its low concentration, low crystallinity, and good dispersion. Acting as an electron shuttle, Ru-AA significantly improved the apparent second-order rate constant (k_{app}) of aniline oxidation from 10.3 to 18.9 M⁻¹ s⁻¹ with its concentration increasing from 0.55 to 2.2 g L⁻¹. Aniline degradation in catalytic oxidation was markedly influenced by pH, and the k_{app} decreased from 314.3 to 3.3 M⁻¹ s⁻¹ with increasing pH from 4.0 to 9.0. The intermediates of aniline in the catalytic permanganate oxidation were determined by LC-MS/MS analysis. Ru-AA displayed an excellent stability in first 10 consecutive runs, and the regenerated Ru-AA showed a better performance than the spent one after 15 runs, but less catalytic capability than the virgin one due to the leaching of Ru. The schematic mechanism for Ru-AA-catalyzed permanganate oxidation of aniline was proposed finally.

Keywords: Aniline; Kinetics; Catalysis; Byproduct; Pathway

1. Introduction

Permanganate oxidation already has been widely used in water utilities over the past decades for the control of dissolved Mn(II), taste and odor compounds, and cyanotoxins, due to its comparative stability, ease of handling, and relatively low cost [1–3].

In recent years, the potential application of permanganate for oxidative removal of emerging pollutants during water and wastewater treatment has received great attention [4–6]. Jiang et al. reported that permanganate was much more effective for the oxidative removal of phenolic endocrine-disrupting chemicals in real water at pH 8.0 compared to ozone, chlorine, and

*Corresponding author.

ferrate, mainly due to its relatively high stability as well as selectivity therein [5]. But considering the unpleasant color of permanganate, only very low inlet concentration was allowed to avoid the appearance of chromaticity in the treated water. Thus, catalyzing this process is becoming a necessity to achieve high organics removal with low permanganate dosage.

Among the catalysts which have potential for use in selective oxidations, ruthenium (Ru) takes a special position owing to its versatility. Ru can catalyze numerous oxidative transformations: the oxidation of alkanes, the cleavage of double bonds, the asymmetric epoxidation of alkenes, the oxidation of alcohols and ethers, and the oxidation of amines and phenols [7–9]. Nandibewoor and his colleagues had extensively investigated Ru^{III}-catalyzed permanganate oxidation process either under strongly alkaline ($[\text{OH}^-] \geq 0.05 \text{ M}$) or strongly acidic ($[\text{H}^+] \geq 0.03 \text{ M}$) conditions [10–13]. Ru^{III} was shown to be an excellent catalyst for permanganate oxidation of amino acids (L-leucine, L-isoleucine, and L-arginine) [10,11], atenolol [12], and D-panthenol [14] under strong alkaline conditions, and of amitriptyline-A tricyclic antidepressant drug under strong acidic conditions [13]. However, all previous studies employed soluble Ru^{III} to catalyze permanganate oxidation. Ru is rather expensive and the addition of Ru^{III} into permanganate oxidation system is far from practical application since it is troublesome to remove or/and recover Ru from the effluents. Heterogeneous catalysts, especially solid oxide-based ones, can overcome those disadvantages of homogeneous catalysts. Therefore, a ceria-supported ruthenium nanoparticles (Ru/CeO₂) was synthesized in our previous study to catalyze the oxidation of butylparaben by permanganate [6]. The presence of 1.0 g L⁻¹ Ru/CeO₂ increased the oxidation rate of butylparaben by 3–96 times at pH 4.0–8.0. Ru/TiO₂ was further synthesized to catalyze permanganate oxidation for degrading emerging pollutants with various organic moieties [15]. The presence of 1.0 g L⁻¹ Ru/TiO₂ increased the second-order reaction rate constants of bisphenol A, diclofenac, acetaminophen, sulfamethoxazole, benzotriazole, carbamazepine, butylparaben, ciprofloxacin, and aniline by 0.3–119 times at pH 7.0 [15]. Although satisfactory performance was observed in previous studies, the particle sizes of CeO₂ and TiO₂ were lower than 10–50 μm, which would lead to difficult separation of catalysts from aqueous solution. Therefore, ball-shaped activated alumina (AA) with an average diameter of 3–4 mm was employed as support in preparation of catalyst Ru-AA in this study, and the catalytic performance of Ru-AA in permanganate oxidation was evaluated for the first time.

According to the US EPA, aniline is released into the environment primarily from its industrial uses as a chemical intermediate in the production of polymers, pesticides, pharmaceuticals, and dyes [16]. Aniline in solution adsorbs strongly to colloidal organic matter, which effectively increases its solubility and movement into surface and groundwater. It is thus a very significant route of environmental pollution which puts human health and aquatic organisms at risk. Considerable concerns exist over the loss of aniline to the environment during production processes or incomplete treatment of industrial waste streams [17], since it was identified as a potential carcinogen [18]. Being extremely toxic (EPA suggested limit in water is 0.262 mg L⁻¹ [19]), aniline should be efficiently decomposed to prevent water pollution. Therefore, aniline was employed as the target contaminant in this study.

Homogeneous permanganate oxidation with Ru³⁺ as catalyst was highly dependent on pH and the dosage of catalyst [6,20,21]. The removal of target contaminant decreased gradually with increasing pH due to the lower formation of Ru^{VII} or Ru^{VI} from Ru^{III} at higher pH. It has been proved that Ru^{VII} or Ru^{VI} played a role of co-oxidant to decompose organics at circumneutral pH [6,21]. While the pH and catalyst dosage influences on Ru-AA-catalyzed permanganate oxidation of aniline were still poorly understood. In our previous study, the byproducts of aniline in permanganate oxidation and Ru³⁺-catalyzed permanganate oxidation were detected by LC-MS/MS [21]. But the degradation pathways of aniline in the presence of permanganate and Ru-AA were still unexplored. The stability and reusability of catalyst are critical in catalytic reactions, especially for practical applications, thus it is important to investigate the stability of Ru-AA by reusing it in successive runs and to examine its performance after regeneration. Therefore, the objective of this work was to study the kinetics of aniline oxidation by Ru-AA-catalyzed permanganate, to identify the intermediate products of aniline, to assess the stability of virgin and spent Ru-AA in consecutive runs, and to propose the possible schematic mechanism based on all the above mentioned studies.

2. Materials and experiments

2.1. Materials

Aniline, KMnO₄, NH₂OH·HCl, and AA of reagent grade were purchased from Tianjin Chemicals Reagent Co. Ltd, and used without further purification. The KMnO₄ crystals were dissolved in deionized water to make a 10 mM stock solution. The stock solution of

aniline (1 mM) or $\text{NH}_2\text{OH}\cdot\text{HCl}$ (scavenger) (0.1 M) was prepared by dissolving a predetermined quantity of aniline or $\text{NH}_2\text{OH}\cdot\text{HCl}$ in deionized water. The eluents in HPLC and LC–MS/MS analyses were of chromatographic purity and used without further purification. Filters used were Millipore Millex syringe-driven 0.22- μm (pore size) cellulose acetate membrane filters.

2.2. Catalyst preparation and characterization

The catalyst samples containing 0.5 wt% of Ru were prepared by incipient-wetness impregnation of AA (diameter: 3–4 mm) with an aqueous solution of $\text{RuCl}_3\cdot x\text{H}_2\text{O}$ (Acros Organics), whose concentration was accurately determined by ICP-AES (ICP-Agilent 720ES) before impregnation [22]. The AA support was impregnated at room temperature with an appropriate volume of solution containing the Ru salt to obtain 0.5 wt% Ru contents. After the impregnation step, the catalyst precursors were washed with deionized water for several times, and then dried at 40°C in a vacuum drying oven.

The morphology of Ru-AA was observed with scanning electronic microscope (SEM, Quanta 200F, FEI, US). The energy-dispersive X-ray spectroscopy (EDAX) analysis was also performed in the SEM analysis on Ametek Genesis XM (US) in order to identify the presence of Ru on the surface of support. In order to clarify the valence of Ru on AA, the X-ray photoelectron spectrum (XPS) of Ru-AA was collected on a PHI 500 ESCA System (Perkin-Elmer, US) using monochromatic Al $K\alpha$ radiation (225 W, 15 mA, 1,486.6 eV). X-ray diffraction (XRD) patterns of AA and catalyst samples were obtained on a PANalytical X'Pert PRO Materials Research Diffractometer (PANalytical B.V., Netherland) using Cu $K\alpha$ radiation ($\lambda = 0.15406$ nm). Crystalline phases were identified by comparison with PDF standards from the International Centre for Diffraction Data (ICDD).

2.3. Experimental procedures

All batch experiments on the kinetics of aniline oxidation by permanganate in the presence or absence of Ru-AA were conducted in stoppered conical flasks. In a typical experiment, conical flasks containing 100 mL of aniline, Ru-AA, and 30 mM NaCl (as background electrolyte) were put in water bath for at least 30 min to ensure the temperature of the reactant was 25°C. The experiments were initiated after addition of an aliquot of permanganate stock solution into the reactor. Then the glass caps were tightly plugged and

the flasks were placed on a rotary shaker and covered with a lid to keep in the dark during the whole reaction. Samples were withdrawn at fixed time intervals, filtered through 0.22- μm membrane, and transferred to small beakers containing 100 μL of $\text{NH}_2\text{OH}\cdot\text{HCl}$ (0.1 M) to terminate the reaction. Then, the concentration of residual aniline was determined by HPLC immediately. No buffer was used at pH 4.0–7.0, while borate buffer was used at pH 8.0–9.0. The pH values remained constant during the whole process by adding HCl or NaOH if necessary. The background electrolyte NaCl had negligible effect on aniline degradation (data not shown). All experiments were run in duplicates or triplicates, and all points in the figures are the mean of the results and error bars represent standard deviation of the means.

To assess the stability of Ru-AA, 15 successive experiments were conducted at pH 7.0. The samples collected at the end of reactions were filtered with 0.22- μm membrane filters, and the collected Ru-AA catalyst was washed with deionized water, dried in vacuum at 40°C and then reused in the next cycle. The filtrate was terminated by $\text{NH}_2\text{OH}\cdot\text{HCl}$ immediately and analyzed by HPLC to determine the concentration of residual aniline. To evaluate the leaching of Al from Ru-AA during the successive runs, 0.11 g of Ru-AA was dispersed in 100 mL reaction solution, and then the experiments were initiated after adding 50 μM permanganate at pH 7.0. After shaking for 30 min in the rotary shaker, the reaction was terminated by $\text{NH}_2\text{OH}\cdot\text{HCl}$ (0.1 M), and then the solution and Ru-AA were separated by filtration. In order to precisely quantify the amount of leached Al with ICP-AES, the leachate obtained as stated above, was heated to $\sim 90^\circ\text{C}$ with 2 droplets of concentrated nitric acid until the solution volume was reduced to ~ 5 mL. Then the concentrated leachate was re-diluted to 10 mL for ICP-AES analysis.

Regeneration of the spent catalyst after 15 successive runs was performed by immersing it in the $\text{NH}_2\text{OH}\cdot\text{HCl}$ solution for about 10 min, then the catalyst was collected by filtration and dried in vacuum at 40°C. To examine the possible generation of bromate in Ru-AA-catalyzed permanganate oxidation process, 0.5 mg L^{-1} Br^- was spiked into the aniline bearing solution before the reaction was initiated.

2.4. Analytical methods

Aniline concentration was measured by HPLC (Waters e2695, US) equipped with a C18 column (2.1 mm \times 150 mm, 3.5 μm), while the mobile phase was a mixture of 65% methanol and 35% H_2O and UV

detector was set at 254 nm. Ultra performance liquid chromatography together with electrospray-ionization quadruple time-of-flight tandem mass spectrometry (UPLC-ESI-QTOF MS), Waters Acquity UPLC-Xevo G2 QTOF, was used to detect the intermediates of aniline degradation. In this study, the mass spectrometer was operated in the m/z 50–500 range for LC-MS/MS. The eluent was delivered at 0.5 mL min^{-1} by a gradient system (Table 1) from UPLC and partitioned by a Waters column Acquity UPLC BEH C18 column $2.1 \text{ mm} \times 100 \text{ mm}$, $1.7 \mu\text{m}$. The Ru contents of freshly synthesized Ru-AA and Ru-AA used after 15 successive experiments were determined by ICP-AES after microwave digestion in nitric acid. The detection limit of this method was 0.01 mg L^{-1} for Ru. Bromide and bromate were analyzed using a reagent-free ion chromatography system (ICS-3000, Dionex) coupled with a conductivity detector. A high-capacity hydroxide-selective analytical column (AS19, $4 \times 250 \text{ mm}$, Dionex) and its respective guard column (AG19, $4 \times 50 \text{ mm}$, Dionex) were used for separation. The Brunauer–Emmett–Teller (BET) specific surface area was measured by the N_2 gas adsorption method on an ASAP analyzer (Micromeritics, USA). Aniline mineralization (TOC removal) was examined with a TOC II analyzer (Elementar). In order to ensure the accurate measurement of TOC, the concentrations of aniline, permanganate, and Ru-AA were enlarged by 5-fold, respectively.

3. Results and discussion

3.1. Characterization of Ru catalyst

The morphologies of AA, virgin Ru-AA, and Ru-AA used after one time and 10 times were characterized by SEM, as shown in Fig. 1. The large-scale images showed no obvious difference in surface structure, indicating that ruthenium hydroxide coating on the surface of AA was uniform, while the high-resolution micrographs revealed some subtle differences. The surface of virgin AA was composed of many small particles, leading to a rough and porous surface. After incipient-wetness impregnation, some bigger uniformed congeries appeared accompanied by the

loss of small particles. The EDAX analysis performed on the surface of Ru-AA proved the existence of Ru on Ru-AA, although its content was much lower than that of Al and O (Table 2). After 10 consecutive runs, Mn was detected in EDAX analysis, indicating that MnO_2 , the reduction product of permanganate at near neutral pH, was deposited onto the surface of Ru-AA during catalytic oxidation.

The XRD patterns for AA, virgin Ru-AA, and Ru-AA used after one time and 10 times were examined in Fig. 2. The strong and sharp XRD reflection peaks suggested that AA was well crystallized. AlOOH was believed to be the major crystalline phase as indicated by the diffraction peaks at 13.8° , 28.3° , 38.3° , 49.0° , and 64.7° . These peaks corresponded to five indexed planes (0 2 0), (1 2 0), (0 3 1), (2 0 0), and (1 5 1) of AlOOH , respectively [23,24]. The XRD patterns for AA were not affected by the impregnation of ruthenium hydroxide, as the peak of Ru was not observed, due to its low concentration, low crystallinity, and good dispersion. The peak intensity for Ru-AA used after 10 times decreased obviously compared to its virgin counterpart, which was attributed to the coating of MnO_2 onto the surface of Ru-AA during oxidation.

The oxidation state of Ru on virgin Ru-AA and Ru-AA used after 1 time, 2 times, and 10 times was investigated by XPS. It can be seen from Fig. 3 that the characteristic Ru3d peak (right peak) was very near to the C1s peak at 284.6 eV (left peak). According to the fitting results, the main Ru species on the surface corresponds to Ru^{III} with a well-defined peak at 281.0 eV [25]. However, the intensity of Ru^{III} peak decreased with increasing repeated use, which confirmed the deposition of MnO_2 onto the surface of Ru-AA. The XPS scanning for Mn was also performed (Fig. 4), and the characteristic $\text{Mn}2\text{p}_{1/2}$ and $\text{Mn}2\text{p}_{3/2}$ peak at 653.8 and 642.2 eV were well defined, indicating that the main manganese species on the surface of Ru-AA corresponds to MnO_2 [25].

BET measurements showed that the synthesized Ru-AA had a specific surface area of $203 \text{ m}^2 \text{ g}^{-1}$, which was lower than that of AA ($272 \text{ m}^2 \text{ g}^{-1}$). The decrease in specific surface might be caused by mouth blockage during the impregnation of ruthenium hydroxide. The diameter of Ru-AA was 3–4 mm, which was almost the same as that of AA, indicating that the impregnation layer had barely impact on the size of supports.

3.2. Catalytic performance of Ru-AA

Aniline oxidation by permanganate in the absence and presence of Ru-AA was investigated in batch experiments in order to evaluate the catalytic

Table 1
Details of the LC-MS/MS gradient program

Time (min)	Milli-Q water (%)	Methanol (%)
0	99	1
0.5	99	1
10	10	90
11	10	90
12	99	1

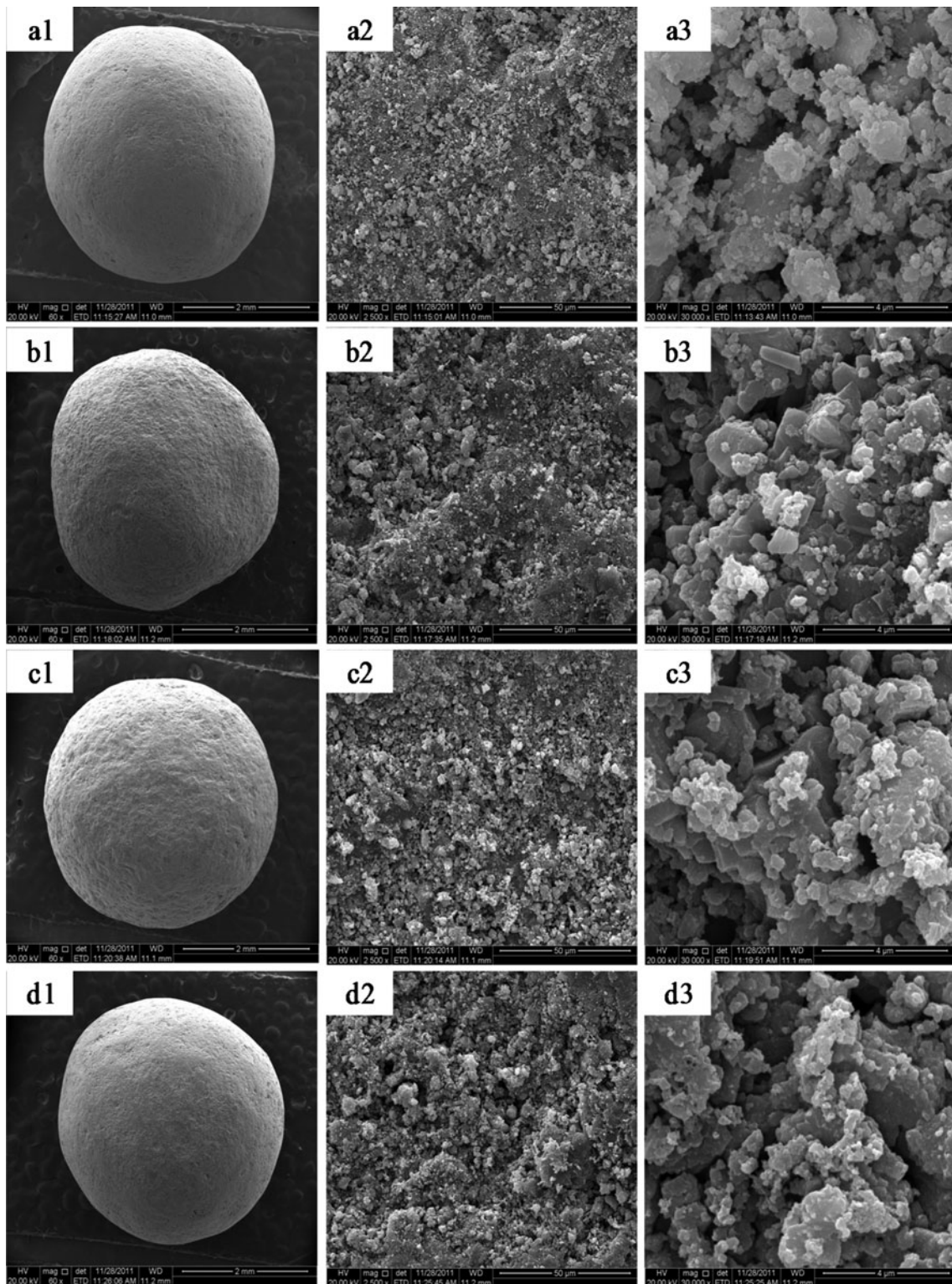


Fig. 1. SEM images for (a1) AA, 60 \times , (a2) AA, 2,500 \times , (a3) AA, 30,000 \times , (b1) virgin Ru-AA, 60 \times , (b2) virgin Ru-AA, 2,500 \times , (b3) virgin Ru-AA, 30,000 \times , (c1) Ru-AA used after one time, 60 \times , (c2) Ru-AA used after one time, 2,500 \times , (c3) Ru-AA used after one time, 30,000 \times , (d1) Ru-AA used after ten times, 60 \times , (d2) Ru-AA used after ten times, 2,500 \times , and (d3) Ru-AA used after ten times, 30,000 \times .

Table 2
EDAX elemental microanalysis of AA and Ru-AA (zones identified in Fig. 1(a3), (b3), and (d3))

	Content of the elements (%)			
	Al	O	Ru	Mn
AA	54.25	45.75	–	–
Virgin Ru-AA	46.64	51.36	2.00	–
Ru-AA used after ten times	47.16	43.71	1.16	7.97

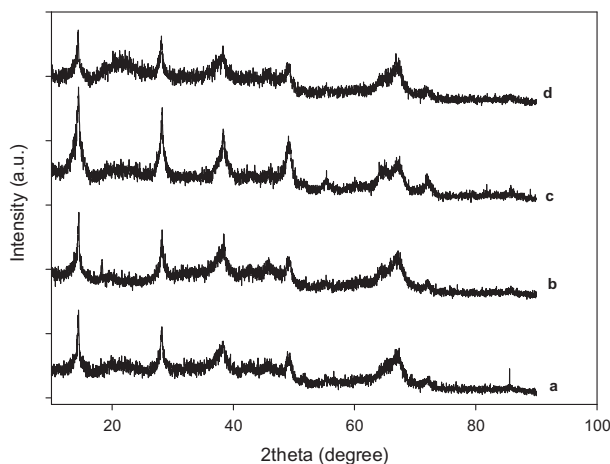


Fig. 2. XRD patterns for (a) AA, (b) virgin Ru-AA, (c) Ru-AA used after one time, and (d) ten times.

efficiency of Ru-AA, and the results are shown in Fig. 5. With the application of 0.55 g L^{-1} Ru-AA, the removal of aniline by permanganate oxidation was increased from $42.5 \pm 0.3\%$ to $53.0 \pm 1.3\%$, at the end of 20 min reaction. Since Ru-AA exerted negligible aniline adsorption, and AA had no or very weak catalytic effect on aniline oxidation, Ru doped on the surface of AA was the active ingredient responsible for the improved aniline oxidation by permanganate.

Fig. 6 shows the time courses of oxidative degradation of aniline by permanganate in 10-fold excess in the presence of Ru-AA. As can be seen, the loss of aniline followed the pseudo-first-order kinetics within the time scales investigated, suggesting that the reaction was first-order with respect to aniline. According to Zhang et al. [21], when permanganate was in 10-fold excess, the oxidation kinetics of aniline by permanganate can be described by a second-order rate law:

$$-\frac{d[\text{Aniline}]}{dt} = k_{\text{obs}}[\text{Aniline}] = k_{\text{app}}[\text{Mn(VII)}][\text{Aniline}] \quad (1)$$

where k_{obs} and k_{app} are the first- and second-order rate constants, respectively. With increasing Ru-AA dosage from 0.55 to 2.2 g L^{-1} , the apparent second-order rate constant ($k_{\text{app}}, \text{M}^{-1} \text{ s}^{-1}$) increased linearly from 10.3 to $18.9 \text{ M}^{-1} \text{ s}^{-1}$, as shown in Fig. 6(a) and (b), suggesting a first-order dependence of the k_{app} on the dosage of Ru-AA. However, with further increasing Ru-AA from 2.2 to 2.75 g L^{-1} , k_{app} decreased slightly from 18.9 to $17.8 \text{ M}^{-1} \text{ s}^{-1}$. This can be explained by the catalytic mechanism of Ru-AA in permanganate oxidation. In previous study, the *in situ* XANES analysis revealed that heterogeneous Ru^{III} catalyst acted as an electron shuttle in permanganate oxidation [6]. Ru^{III} deposited on the surface of catalyst was oxidized by permanganate to its higher oxidation state Ru^{VII} and Ru^{VI} , which acted as the co-oxidants. Then, Ru^{VII} and Ru^{VI} were reduced by organics to its initial state of Ru^{III} [6]. Therefore, excessive Ru-AA may exert a significant demand for permanganate, reduce the available oxidant for aniline destruction, and decrease the apparent second-order rate constant. As shown in Fig. 7, aniline degradation by Ru-AA-catalyzed permanganate exhibited strong pH dependence. The oxidation rates of aniline in catalytic process dropped progressively from 316.0 to $4.1 \text{ M}^{-1} \text{ s}^{-1}$ with pH increasing from 4.0 to 9.0 due to the decrease in oxidation–reduction potential of permanganate and the reduced formation of Ru^{VII} or Ru^{VI} [6,15].

The rate constants for the reaction of aniline with permanganate in the presence and absence of Ru-AA were compared with that obtained with selective oxidants (Fe(VI) , $6.63 \times 10^3 \text{ M}^{-1} \text{ s}^{-1}$; HClO , $4.46 \times 10^4 \text{ M}^{-1} \text{ s}^{-1}$; ClO_2 , $4.48 \times 10^5 \text{ M}^{-1} \text{ s}^{-1}$, and O_3 , $1.39 \times 10^7 \text{ M}^{-1} \text{ s}^{-1}$) and non selective oxidant ($\cdot\text{OH}$, $1.00 \times 10^{10} \text{ M}^{-1} \text{ s}^{-1}$) at pH 7.0 [26]. It was obvious that Ru-AA-catalyzed permanganate showed higher activity to aniline than permanganate alone, but was less reactive than other oxidants. However, aniline degradations with other oxidants also suffer some demerits. Chlorine (i.e. HOCl) could react with aniline to generate chlorine-substituted aniline [27], which might possess higher toxicity than its mother compound, while O_3 could also react with Br^- to generate carcinogenic bromate [28]. Hydroxyl radicals, susceptible to reacting with organic molecules indiscriminately, can be easily consumed by the matrix components, including humic acid and HCO_3^- [29]. On the other hand, Ru-AA-catalyzed permanganate may be advantageous in treating compounds containing anilino-group in real water since it will not form chlorinated byproducts. Moreover, bromate was not detected in the process of aniline oxidation by Ru-AA-catalyzed permanganate when $0.5 \text{ mg L}^{-1} \text{ Br}^-$ was

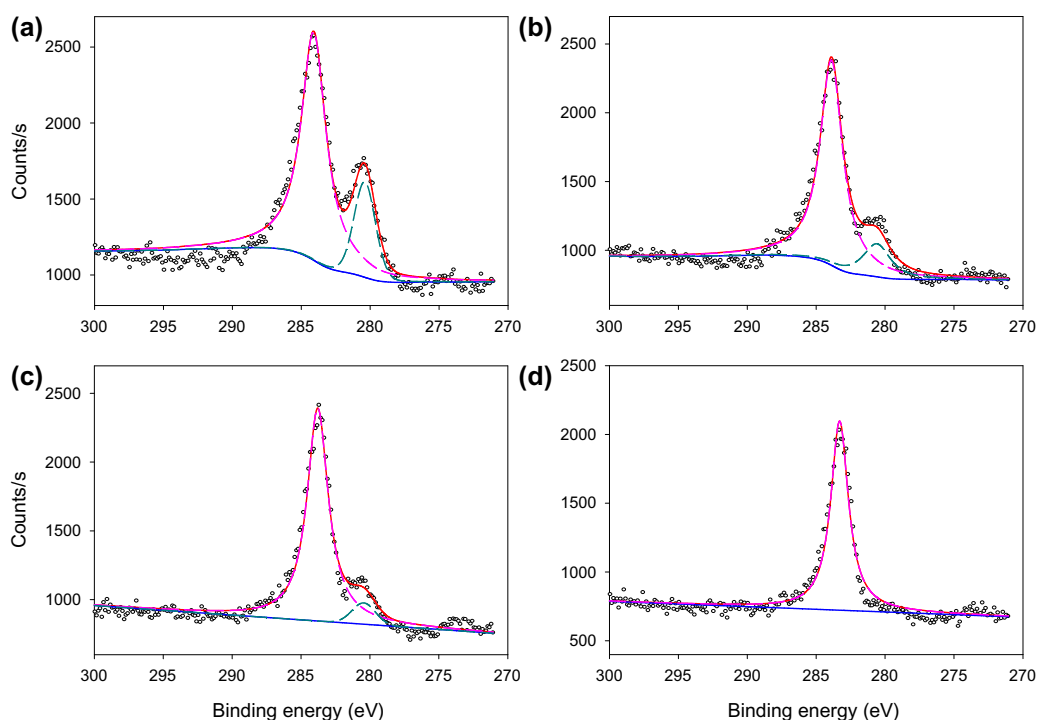


Fig. 3. Ru3d and C1s XPS for (a) virgin Ru-AA, (b) Ru-AA used after one time, (c) two times, and (d) ten times.

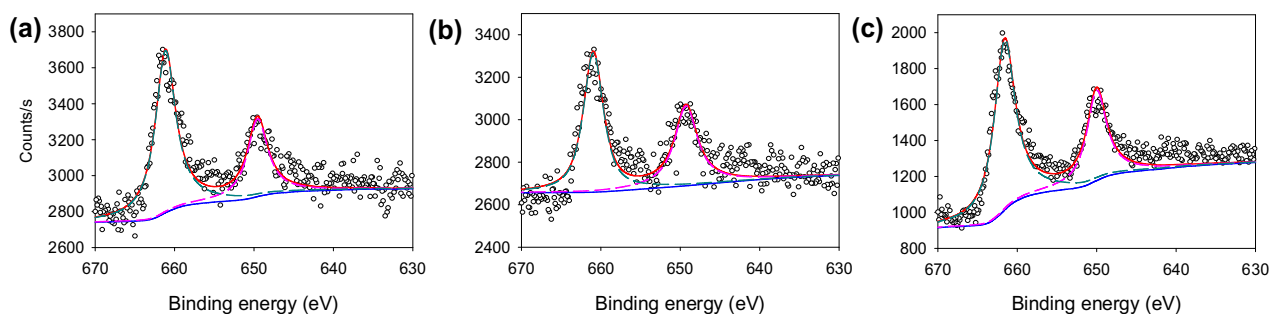


Fig. 4. Mn2p XPS for (a) Ru-AA used after one time, (b) two times, and (c) ten times.

spiked into the sample before the reaction started. Therefore, Ru-AA-catalyzed permanganate oxidation is a promising way to decompose aniline in aqueous solution, although the degradation rate was lower compared with other oxidative processes.

3.3. Stability of Ru-AA in ten consecutive runs

Since the stability and reusability of the catalyst are critical in catalyzed reactions, especially for practical industrial applications, the stability of the Ru-AA catalyst was investigated by reusing catalyst in 15 successive experiments under same reaction conditions and the results are shown in Fig. 8. Aniline removal

in the first 10 cycles remained almost constant, but decreased progressively from $66.9 \pm 0.5\%$ to $41.5 \pm 1.5\%$ from the tenth to fifteenth run. After fifteen cycles, the mass content of Ru in Ru-AA decreased slightly from $0.50 \pm 0.02\%$ to $0.46 \pm 0.01\%$, and the Mn in the catalyst was determined to be 0.1%, due to the deposition of MnO_2 on the Ru-AA surface. It should be noted that MnO_2 had no catalytic and adsorptive effect for aniline at pH 7.0, according to previous studies [6,15]. The leached Al desorbed from Ru-AA at the end of successive runs was lower than 0.1 mg L^{-1} . Compared to the progressively decreasing performance of Ru/ CeO_2 in the consecutive oxidation, Ru-AA displayed an excellent stability, although the

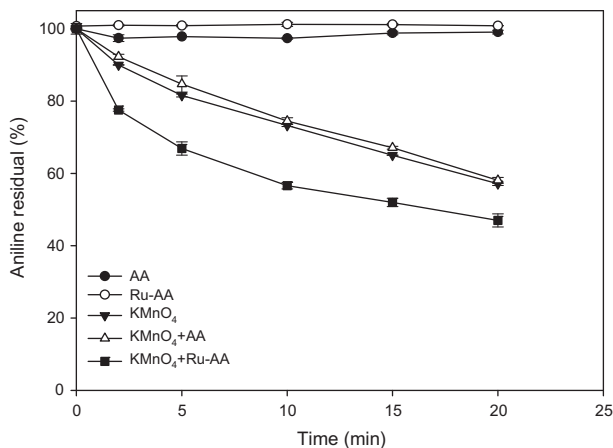


Fig. 5. The negligible adsorption effects of AA (0.55 g L^{-1}) and Ru-AA (0.55 g L^{-1}) for aniline ($5 \mu\text{M}$) and the catalytic effects of AA (0.55 g L^{-1}) and Ru-AA (0.55 g L^{-1}) in permanganate ($50 \mu\text{M}$) oxidation of aniline ($5 \mu\text{M}$) at $\text{pH } 7.0 \pm 0.1$ and $T = 25^\circ\text{C}$.

deposited MnO_2 depressed the catalytic performance of Ru-AA by masking the active sites of Ru-AA since the eleventh run [6]. The excellent stability of Ru-AA would favor its practical application in pilot or engineering practice. In addition, the particle size of Ru-AA was much larger than that of Ru/ CeO_2 [6] and Ru/ TiO_2 [15], thus it would be much easier to separate Ru-AA from the aqueous solution.

The stability and reusability of spent Ru-AA (used in the consecutive experiment as mentioned above) after regeneration by $\text{NH}_2\text{OH}\cdot\text{HCl}$ was examined and the removal of aniline is shown in Fig. 8. $\text{NH}_2\text{OH}\cdot\text{HCl}$ would reduce the deposited MnO_2 on the surface of Ru-AA to Mn^{2+} , thus the deactivated Ru-AA could be

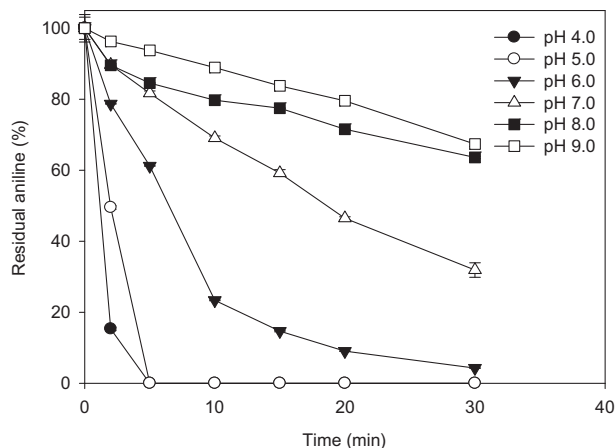


Fig. 7. Influence of pH on Ru-AA-catalyzed permanganate oxidation of aniline. Reaction conditions: $[\text{aniline}]_0 = 5 \mu\text{M}$, $[\text{KMnO}_4]_0 = 50 \mu\text{M}$, $[\text{Ru-AA}] = 1.1 \text{ g L}^{-1}$, and $T = 25^\circ\text{C}$.

regenerated. After regeneration, Ru-AA displayed better performance than its counterpart used after 15 runs, but a 10% decrease in aniline removal was observed in comparison to that with the fresh catalyst. This may be caused by the leaching of Ru during regeneration, which was decreased from 0.46 to 0.38%. Generally speaking, the regenerated Ru-AA maintained a satisfied stability in the 10 successive runs with an average removal of 52.5% for aniline.

3.4. Mineralization of aniline and degradation pathways

In the advanced oxidation of aniline, aromatic intermediates have been identified. The existence of free radicals led to the total mineralization of aniline [30,31],

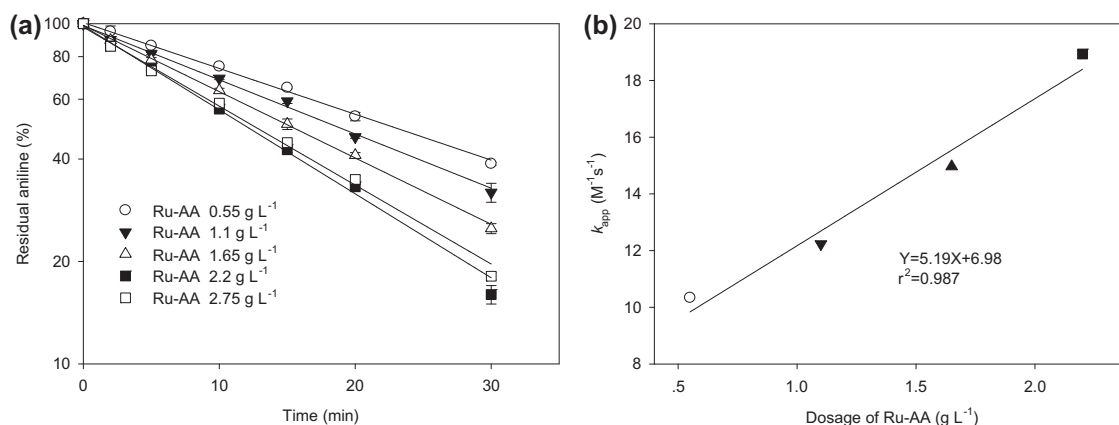


Fig. 6. (a) Influence of Ru-AA dosage on Ru-AA-catalyzed permanganate oxidation of aniline and (b) the linearity between the second-order rate constants (k_{app}) and dosage of Ru-AA. Reaction conditions: $[\text{aniline}]_0 = 5 \mu\text{M}$, $[\text{KMnO}_4]_0 = 50 \mu\text{M}$, $\text{pH } 7.0 \pm 0.1$, and $T = 25^\circ\text{C}$.

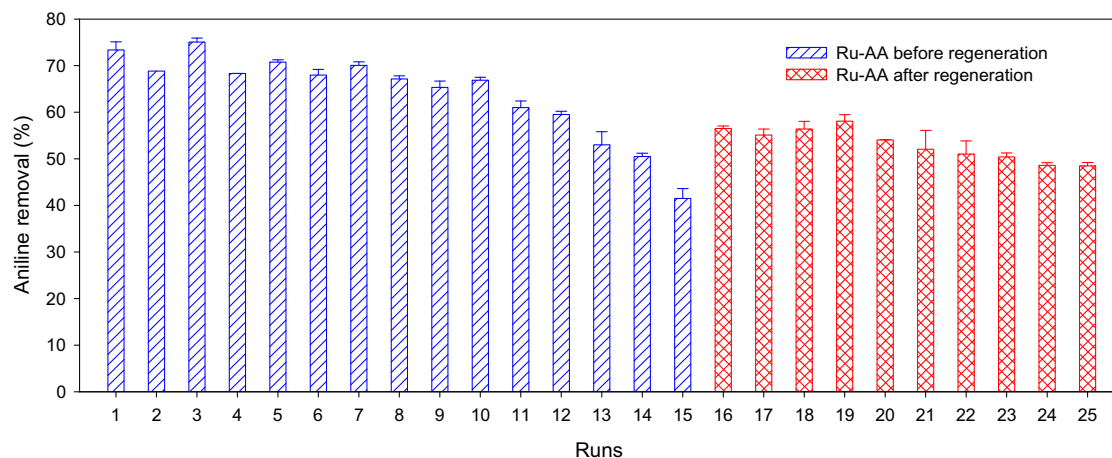


Fig. 8. Removal of aniline by permanganate oxidation in consecutive runs in the presence of fresh Ru-AA and Ru-AA after regeneration. Reaction conditions: $[\text{aniline}]_0 = 5 \mu\text{M}$, $[\text{KMnO}_4]_0 = 50 \mu\text{M}$, $[\text{Ru-AA}] = 1.1 \text{ g L}^{-1}$, $\text{pH } 7.0 \pm 0.1$, $T = 25^\circ\text{C}$, and reaction time = 30 min.

while aniline oxidation by MnO_2 generated azobenzene as the only byproduct at $\text{pH } 4.0$, which agreed with a postulated oxidative-coupling reaction mechanism [32]. Nitroso- and nitro-compound may be yielded when peroxy acid being the oxidant [28,30]. Azo compounds were also one of the most common products in both the electrochemical oxidation and photocatalyzed systems [33–35]. Therefore, different oxidants may exhibit different oxidation mechanisms. In this work, a mechanistic study of aniline oxidation by catalytic permanganate oxidation has been undertaken. Firstly, oxidation products of aniline oxidation have been tentatively identified by LC coupled with a mass spectrometer. The

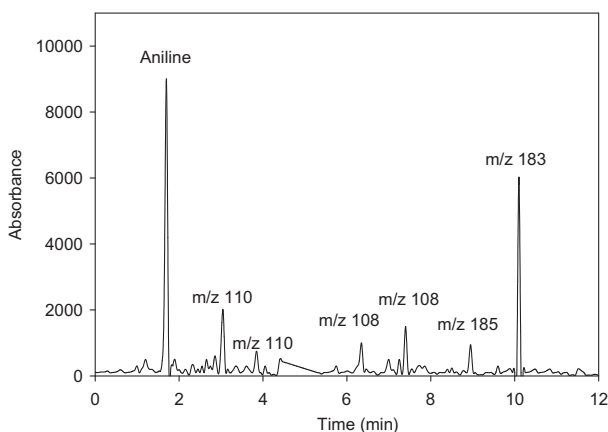


Fig. 9. LC–MS chromatogram for aniline and the intermediates in catalytic permanganate oxidation. Reaction conditions: $[\text{aniline}]_0 = 5 \mu\text{M}$, $[\text{KMnO}_4]_0 = 50 \mu\text{M}$, $[\text{Ru-AA}] = 1.1 \text{ g L}^{-1}$, $\text{pH } 7.0 \pm 0.1$, $T = 25^\circ\text{C}$, and reaction time = 30 min.

formation of each degradation compounds has been rationalized taking into account the knowledge concerning permanganate, Ru^{VII} and Ru^{VI} reactivity, and the structure of aniline. Six byproducts were detected and structures for these products were proposed upon the basis of (i) the masses of pseudo-molecular ions $[\text{M} + \text{H}]^+$, (ii) the major fragments of the MS/MS spectra, and (iii) previously well-reported information on product formation during the oxidative processes of Ag^+ -loaded TiO_2 [34] and homogeneous Ru^{III} -catalyzed permanganate [21]. Most of the byproducts had greater molecular weights than their parent molecule and the degradation pathways were proposed in Figs. 9 and 10. It was very hard to distinguish the retention times for the isomers, e.g. m/z 110 and 108, and thus the retention time for each byproduct was not offered. The proposed structures of degradation products revealed that permanganate and Ru^{VII} or Ru^{VI} mainly attacked the aromatic ring, leading to the formation of various hydroxyl-substituted aniline, as shown in Fig. 10. Another pathway with the formation of azobenzene indicated that the oxidative-coupling reaction mechanism [32] also existed in permanganate oxidation in the presence of Ru-AA. Sanchez et al. [36] and Piccinini et al. [37] found that during the mineralization of aniline in photocatalysis, organic nitrogen was transformed into the corresponding inorganic form (NH_4^+ , NO_2^- , and NO_3^-). However, in this study none of the NH_4^+ , NO_2^- , and NO_3^- was detected by ion chromatography due to the mild oxidizability of Ru-AA-catalyzed permanganate.

It should be noted that the degradation products in Ru-AA-catalyzed permanganate oxidation were completely identical to those obtained in homoge-

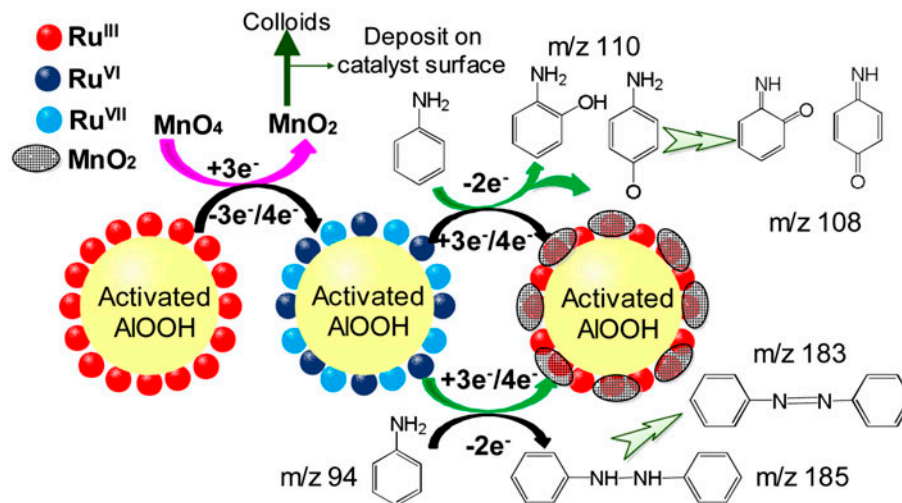


Fig. 10. Proposed mechanisms for Ru-AA-catalyzed permanganate oxidation of aniline.

neously catalytic permanganate with Ru^{III} [21], which confirmed again that Ru^{III} was the real catalytic component. The catalytic mechanisms of Ru-AA in aniline oxidation by permanganate were proposed based on LC-MS/MS results, the role of Ru in permanganate oxidation reported in previous studies [6,15] and the stability of Ru-AA in consecutive runs, and shown in Fig. 10.

The mineralization rate of aniline was much slower than its disappearance rate in Ru-AA-catalyzed permanganate oxidation, as shown in Figs. 7 and 11. Only $11 \pm 1.6\%$ – $46 \pm 1.8\%$ of aniline was mineralized by catalytic permanganate oxidation in 30 min over the pH

range of 4.0–7.0, whereas little mineralization occurred at pH 8.0–9.0. This phenomenon implied that some degradation products of aniline were resistant to Ru-AA-catalyzed permanganate oxidation. Therefore, although aniline was effectively removed by Ru-AA-catalyzed permanganate oxidation, the newly formed byproducts should be paid attention and further techniques were needed in order to achieve complete mineralization.

4. Conclusions

Ruthenium hydroxide loaded onto AA was synthesized for the first time and proved to be effective for catalyzing aniline oxidation by permanganate. The virgin and spent Ru-AA were characterized by SEM-EDAX, BET, XRD, and XPS. Although SEM-EDAX proved the existence of Ru on the surface of AA, XRD patterns for AA were not affected by the impregnation of ruthenium hydroxide, due to its low concentration, low crystallinity, and good dispersion. The impregnation of ruthenium hydroxide led to a decrease in specific surface by mouth blockage. Ru-AA, acting as an electron shuttle, significantly improved the apparent second-order rate constant of aniline oxidation from 10.3 to $18.9 \text{ M}^{-1} \text{ s}^{-1}$, with its concentration increasing from 0.55 to 2.2 g L^{-1} . The performance of Ru-AA was markedly influenced by pH, and the degradation of aniline decreased from 314.3 to $3.3 \text{ M}^{-1} \text{ s}^{-1}$ with increasing pH from 4.0 to 9.0. The degradation pathways of aniline in catalytic permanganate oxidation were proposed based on the identification of byproducts of aniline in LC-MS/MS analysis. Ru-AA displayed an excellent stability in 15

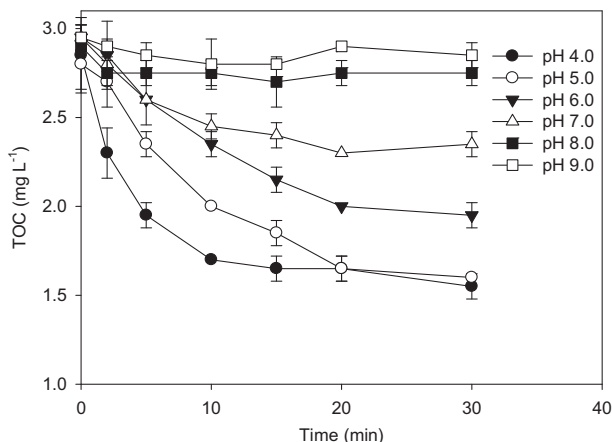


Fig. 11. Mineralization of aniline by permanganate oxidation with Ru-AA as catalyst. Reaction conditions: $[\text{aniline}]_0 = 25 \mu\text{M}$, $[\text{KMnO}_4]_0 = 250 \mu\text{M}$, $[\text{Ru-AA}] = 5.5 \text{ g L}^{-1}$, $T = 25^\circ\text{C}$, and reaction time = 30 min.

consecutive runs, which would favor its practical application in pilot or engineering practice. After regeneration, Ru-AA displayed better performance than its counterpart used after 15 runs, but a 10% decrease in aniline removal was observed in comparison to that with the fresh catalyst. Finally, the catalytic mechanisms of Ru-AA in aniline oxidation by permanganate were proposed based on LC-MS/MS results, the role of Ru in permanganate oxidation, and the stability of Ru-AA in consecutive runs.

Acknowledgements

This work was supported by the China Postdoctoral Science Foundation (2015M571660), the Fundamental Research Funds for the Central Universities (2014B12614), the Foundation of Ministry of Education Key Laboratory of Integrated Regulation and Resource Development on Shallow Lakes, Hohai University, China (2014002), and the Priority Academic Program Development of Jiangsu Higher Education Institutions.

References

- [1] J.E. Van Benschoten, W. Lin, W.R. Knocke, Kinetic modeling of manganese(II) oxidation by chlorine dioxide and potassium-permanganate, *Environ. Sci. Technol.* 26 (1992) 1327–1333.
- [2] A.M. Dietrich, R.C. Hoehn, L.C. Dufresne, L.W. Buffin, D.M.C. Rashash, B.C. Parker, Oxidation of odorous and nonodorous algal metabolites by permanganate, chlorine, and chlorine dioxide, *Water Sci. Technol.* 31 (1995) 223–228.
- [3] E. Rodríguez, A. Sordo, J.S. Metcalf, J.L. Acero, Kinetics of the oxidation of cylindrospermopsin and anatoxin-a with chlorine, monochloramine and permanganate, *Water Res.* 41 (2007) 2048–2056.
- [4] J. Jiang, S.Y. Pang, J. Ma, Oxidation of triclosan by permanganate (Mn(VII)): Importance of ligands and in situ formed manganese oxides, *Environ. Sci. Technol.* 43 (2009) 8326–8331.
- [5] J. Jiang, S.Y. Pang, J. Ma, H.L. Liu, Oxidation of phenolic endocrine disrupting chemicals by potassium permanganate in synthetic and real waters, *Environ. Sci. Technol.* 46 (2012) 1774–1781.
- [6] J. Zhang, B. Sun, X.H. Guan, H. Wang, H.L. Bao, Y.Y. Huang, J.L. Qiao, G.M. Zhou, Ruthenium nanoparticles supported on CeO₂ for catalytic permanganate oxidation of butylparaben, *Environ. Sci. Technol.* 47 (2013) 13011–13019.
- [7] A.K. Singh, A.K. Singh, V. Singh, S. Rahmani, A. Singh, B. Singh, Ru(III) catalysed oxidation of diethanolamine and triethanolamine by Br(V) in presence of perchloric acid, *J. Chem. Res.* (2006) 56–63.
- [8] B. Singh, A.K. Singh, K.L. Singh, R. Dubey, S.K. Singh, Mechanism of Ru(III) catalysis in potassium bromate oxidation of dimethyl sulphoxide in perchloric acid. A kinetic approach, *Oxid. Commun.* 34(3) (2011) 526–532.
- [9] A. Saha, B.C. Ranu, Ruthenium(III)-catalysed phenyl-selenylation of allyl acetates by diphenyl diselenide and indium(I) bromide in neat: Isolation and identification of intermediate, *Org. Biomol. Chem.* 9(6) (2011) 1763–1767.
- [10] A.K. Kini, S.A. Farokhi, S.T. Nandibewoor, A comparative study of ruthenium(III) catalysed oxidation of L-leucine and L-isoleucine by alkaline permanganate. A kinetic and mechanistic approach, *Trans. Metal Chem.* 27(5) (2002) 532–540.
- [11] N.N. Halligudi, S.M. Desai, S.T. Nandibewoor, Free radical intervention, deamination and decarboxylation in the ruthenium(III)-catalysed oxidation of L-arginine by alkaline permanganate—A kinetic study, *Trans. Metal Chem.* 26(1/2) (2001) 28–35.
- [12] G.C. Hiremath, R.M. Mulla, S.T. Nandibewoor, Kinetic, mechanistic and spectral investigation of ruthenium(III) catalysed oxidation of Atenolol by alkaline diperiodatonickelate(IV) (stopped flow technique), *Catal. Lett.* 98(1) (2004) 49–56.
- [13] J.C. Abbar, S.D. Lamani, S.T. Nandibewoor, Ruthenium(III) catalyzed oxidative degradation of amitriptyline-A tricyclic antidepressant drug by permanganate in aqueous acidic medium, *J. Solution Chem.* 40(3) (2011) 502–520.
- [14] R.V. Hosahalli, A.P. Savanur, S.T. Nandibewoor, S.A. Chimatadar, Kinetics and mechanism of uncatalysed and ruthenium(III)-catalysed oxidation of d-panthenol by alkaline permanganate, *Trans. Metal Chem.* 35(2) (2010) 237–246.
- [15] J. Zhang, B. Sun, X.M. Xiong, N.Y. Gao, W.H. Song, E.D. Du, X.H. Guan, G.M. Zhou, Removal of emerging pollutants by Ru/TiO₂-catalyzed permanganate oxidation, *Water Res.* 63 (2014) 262–270.
- [16] L. Oliviero, J. Barbier-Jr., D. Duprez, Wet air oxidation of nitrogen-containing organic compounds and ammonia in aqueous media, *Appl. Catal. B-Environ.* 40 (2003) 163–184.
- [17] G.R. Reddy, V.V. Mahajani, Insight into wet oxidation of aqueous aniline over a Ru/SiO₂ catalyst, *Ind. Eng. Chem. Res.* 44 (2005) 7320–7328.
- [18] M. Fukushima, K. Tatsumi, K. Morimoto, The fate of aniline after a photo-fenton reaction in an aqueous system containing iron(III), humic Acid, and hydrogen peroxide, *Environ. Sci. Technol.* 34 (2000) 2006–2013.
- [19] J. Sarasa, S. Cortes, P. Ormad, R. Gracia, J.L. Ovelleiro, Study of the aromatic by-products formed from ozonation of anilines in aqueous solution, *Water Res.* 36 (2002) 3035–3044.
- [20] J. Zhang, X.H. Guan, Ru(III)-catalyzed permanganate oxidation of bisphenol A, *Desalin. Water Treat.* 52 (2014) 4592–4601.
- [21] J. Zhang, Y. Zhang, H. Wang, X.H. Guan, Ru(III) catalyzed permanganate oxidation of aniline at environmentally relevant pH, *J. Environ. Sci.-China* 26 (2014) 1395–1402.
- [22] A. Pintar, J. Batista, T. Tišler, Catalytic wet-air oxidation of aqueous solutions of formic acid, acetic acid and phenol in a continuous-flow trickle-bed reactor over Ru/TiO₂ catalysts, *Appl. Catal. B: Environ.* 84 (2008) 30–41.
- [23] S.C. Shen, W.K. Ng, L.S.O. Chia, Y.C. Dong, R.B.H. Tan, Morphology controllable synthesis of nanostructured

- boehmite and γ -alumina by facile dry gel conversion, *Cryst. Growth Des.* 12 (2012) 4987–4994.
- [24] M. Zhang, B. Gao, Removal of arsenic, methylene blue, and phosphate by biochar/AlOOH nanocomposite, *Chem. Eng. J.* 226 (2013) 286–292.
- [25] NIST X-ray Photoelectron Spectroscopy Database. Available from: <<http://srdata.nist.gov/xps/Default.aspx>>.
- [26] Y. Lee, U. von Gunten, Oxidative transformation of micropollutants during municipal wastewater treatment: Comparison of kinetic aspects of selective (chlorine, chlorine dioxide, ferrateVI, and ozone) and non-selective oxidants (hydroxyl radical), *Water Res.* 44 (2010) 555–566.
- [27] B.T. Gowda, P.J.M. Rao, K. Jyothi, Kinetics of chlorination of anilines by dichloramine-B in aqueous acetic acid, *Oxid. Commun.* 23 (2000) 255–265.
- [28] U. von Gunten, Ozonation of drinking water: Part I. Oxidation kinetics and product formation, *Water Res.* 37 (2003) 1443–1467.
- [29] E.M. Casbeer, V.K. Sharma, Z. Zajickova, D.D. Dionysiou, Kinetics and mechanism of oxidation of tryptophan by ferrate(VI), *Environ. Sci. Technol.* 47 (2013) 4572–4580.
- [30] L. Sánchez, J. Peral, X. Domènech, Aniline degradation by combined photocatalysis and ozonation, *Appl. Catal. B-Environ.* 19 (1998) 59–65.
- [31] R. Levi, M. Milman, M.V. Landau, A. Brenner, M. Herskowitz, Catalytic wet air oxidation of aniline with nanocasted Mn–Ce-oxide catalyst, *Environ. Sci. Technol.* 42 (2008) 5165–5170.
- [32] S. Farhadi, P. Zaringhadam, R.Z. Sahamieh, Photo-assisted oxidation of anilines and other primary aromatic amines to azo compounds using mercury(II) oxide as a photo-oxidant, *Acta Chim. Slov.* 54 (2007) 647–653.
- [33] Y.J. Li, F. Wang, G.D. Zhou, Y.M. Ni, Aniline degradation by electrocatalytic oxidation, *Chemosphere* 53 (2003) 1229–1234.
- [34] A. Kumar, N. Mathur, Photocatalytic oxidation of aniline using Ag⁺-loaded TiO₂ suspensions, *Appl. Catal. A-Gen.* 275 (2004) 189–197.
- [35] C. Karunakaran, S. Senthilvelan, Photocatalysis with ZrO₂: Oxidation of aniline, *J. Mol. Catal. A-Chem.* 233 (2005) 1–8.
- [36] L. Sgnchez, J. Peral, X. Domknech, Photocatalyzed destruction of aniline in UV-illuminated aqueous TiO₂ suspensions, *Electrochim. Acta* 42 (1997) 1877–1882.
- [37] P. Piccinini, C. Minero, M. Vincenti, E. Pelizzetti, Photocatalytic mineralization of nitrogen-containing benzene derivatives, *Catal. Today* 39 (1997) 187–195.